

See discussions, stats, and author profiles for this publication at: <https://www.researchgate.net/publication/7473529>

# Automated System for Fast and Accurate Analysis of SF 6 Injected in the Surface Ocean

ARTICLE *in* ENVIRONMENTAL SCIENCE AND TECHNOLOGY · DECEMBER 2005

Impact Factor: 5.33 · DOI: 10.1021/es050149g · Source: PubMed

---

CITATIONS

3

---

READS

31

4 AUTHORS, INCLUDING:



**Kitack Lee**

Pohang University of Science and Technology

93 PUBLICATIONS 6,951 CITATIONS

SEE PROFILE



**Miok Kim**

Pohang University of Science and Technology

5 PUBLICATIONS 80 CITATIONS

SEE PROFILE

# Automated System for Fast and Accurate Analysis of SF<sub>6</sub> Injected in the Surface Ocean

CHUL-MIN KOO, KITACK LEE,\*  
MIOK KIM, AND DAE-OK KIM

School of Environmental Science and Engineering, Pohang University of Science and Technology, San 31, Hyoja-dong, Nam-gu, Pohang 790-784, Republic of Korea

This paper describes an automated sampling and analysis system for the shipboard measurement of dissolved sulfur hexafluoride (SF<sub>6</sub>) in surface marine environments into which SF<sub>6</sub> has been deliberately released. This underway system includes a gas chromatograph associated with an electron capture detector, a fast and highly efficient SF<sub>6</sub>-extraction device, a global positioning system, and a data acquisition system based on Visual Basic 6.0/C 6.0. This work is distinct from previous studies (1, 2) in that it quantifies the efficiency of the SF<sub>6</sub>-extraction device and its carryover effect and examines the effect of surfactant on the SF<sub>6</sub>-extraction efficiency. Measurements can be continuously performed on seawater samples taken from a seawater line installed onboard a research vessel. The system runs on an hourly cycle during which one set of four SF<sub>6</sub> standards is measured and SF<sub>6</sub> derived from the seawater stream is subsequently analyzed for the rest of each 1 h period. This state-of-art system was successfully used to trace a water mass carrying *Cochlodinium polykrikoides*, which causes harmful algal blooms (HAB) in the coastal waters of southern Korea. The successful application of this analysis system in tracing the HAB-infected water mass suggests that the SF<sub>6</sub> detection method described in this paper will improve the quality of the future study of biogeochemical processes in the marine environment.

## Introduction

Sulfur hexafluoride (SF<sub>6</sub>) is generated solely from anthropogenic sources. It is an extremely stable gas, with an atmospheric lifetime of about 3200 years (3,4). Time-series measurements of atmospheric SF<sub>6</sub> showed a global mean concentration of about 4 parts/trillion by volume (pptv) and an increment rate of 7% per year (available at <http://www.cmdl.noaa.gov/ccgg/iadv/>). The solubility of SF<sub>6</sub> in surface seawater is low, on the order of 0.5–2 fM (1 fM = 10<sup>-15</sup> mol L<sup>-1</sup>), where these values are for dissolved SF<sub>6</sub> in equilibrium with the atmospheric concentration of ~4 pptv (5).

In principle, SF<sub>6</sub> has several advantages over other substances as a candidate marine patch marker for use in the study of biogeochemical processes occurring in the open ocean. The advantageous characteristics of SF<sub>6</sub> include its low background concentration in the marine environment, high analytical sensitivity relative to fluorescent dyes, non-

toxicity to marine organisms, and inertness. However, establishing a coherent SF<sub>6</sub> patch in the surface mixed layer of the ocean and sampling the evolving patch for a period of days to weeks present several challenges. A key complicating factor is the fact that any tracer injected into the surface mixed layer is subject to a range of physical processes, including horizontal advection, vertical shearing across the mixed layer, diffusion into the pycnocline, and streaking due to surface currents across the mixed layer (6).

During the last two decades, several SF<sub>6</sub> release experiments have been conducted in lakes and the open ocean to determine gas exchange rates at the air–water interface (7) and vertical or lateral mixing rates (8) and to study biogeochemical processes occurring in the surface ocean (9–12). Such experiments involve the release of tens of kilograms of SF<sub>6</sub> into surface waters or onto targeted density surfaces in a small geographic region. The release of SF<sub>6</sub> into a localized area leads to the formation of a small patch of water with dissolved SF<sub>6</sub> concentrations that are several orders of magnitude greater than those produced through equilibrium with the overlying atmospheric SF<sub>6</sub> concentration. The use of SF<sub>6</sub> in open-ocean ecosystem perturbation experiments has considerably advanced our knowledge of biogeochemical processes, through the clear definition of fixed volumes of water for which accurate budget estimates of carbon, nutrients, and biomass can be developed. Examples of such work include experiments to test the iron hypothesis in the equatorial Pacific (9, 10), the Southern Ocean (11), and the North Pacific (12).

The great potential of SF<sub>6</sub> as a marker for tracing water masses in the open ocean is likely to prompt its increasing use in future biogeochemical studies. To facilitate such experiments, a shipboard analytical system is required for the accurate and swift analysis of seawater samples. Documented methods for continuous analysis of SF<sub>6</sub> in air and seawater employ either a sparge-trap (13) or a sparge-trap with vacuum extraction (14). Both of these methods are precise; however, they take at least 2–3 min to extract SF<sub>6</sub> from each seawater sample. In addition, ancillary components are needed to ensure accurate sample volume deliver and to secure the stripped SF<sub>6</sub>.

Another documented method (1, 2) for the extraction of SF<sub>6</sub> from a seawater stream employs a membrane contactor, which enables rapid transfer of dissolved SF<sub>6</sub> from the liquid phase to the gas phase. Although the membrane contactor approach has been used previously in SF<sub>6</sub> extraction (1, 2), its efficiency has not been studied under a range of conditions. The present work tests the performance of the membrane contactor over a wide range of experimental conditions and presents a group of operational settings that ensure optimal efficiency. The results of a SF<sub>6</sub> tracer experiment undertaken in the coastal waters of southern Korea in August 2003 are also briefly discussed.

## Description of the Analytical System

The configuration of the automated system for the rapid extraction of SF<sub>6</sub> from seawater samples and subsequent determination of the equilibrated SF<sub>6</sub> is shown schematically in Figure 1. The automated system includes a gas chromatograph associated with an electron capture detector (GC-ECD), a SF<sub>6</sub>-extraction device, a GPS, and a data integration and visualization system. This automated system operates on an hourly cycle, during which one set of four gaseous SF<sub>6</sub> standards is measured and SF<sub>6</sub> derived from the seawater stream is progressively analyzed for the rest of each hourly cycle. Under the control of a Visual Basic 6.0/C 6.0-based

\* Corresponding author phone: 82-54-279-2285; fax: 82-54-279-8299; e-mail: ktl@postech.ac.kr.

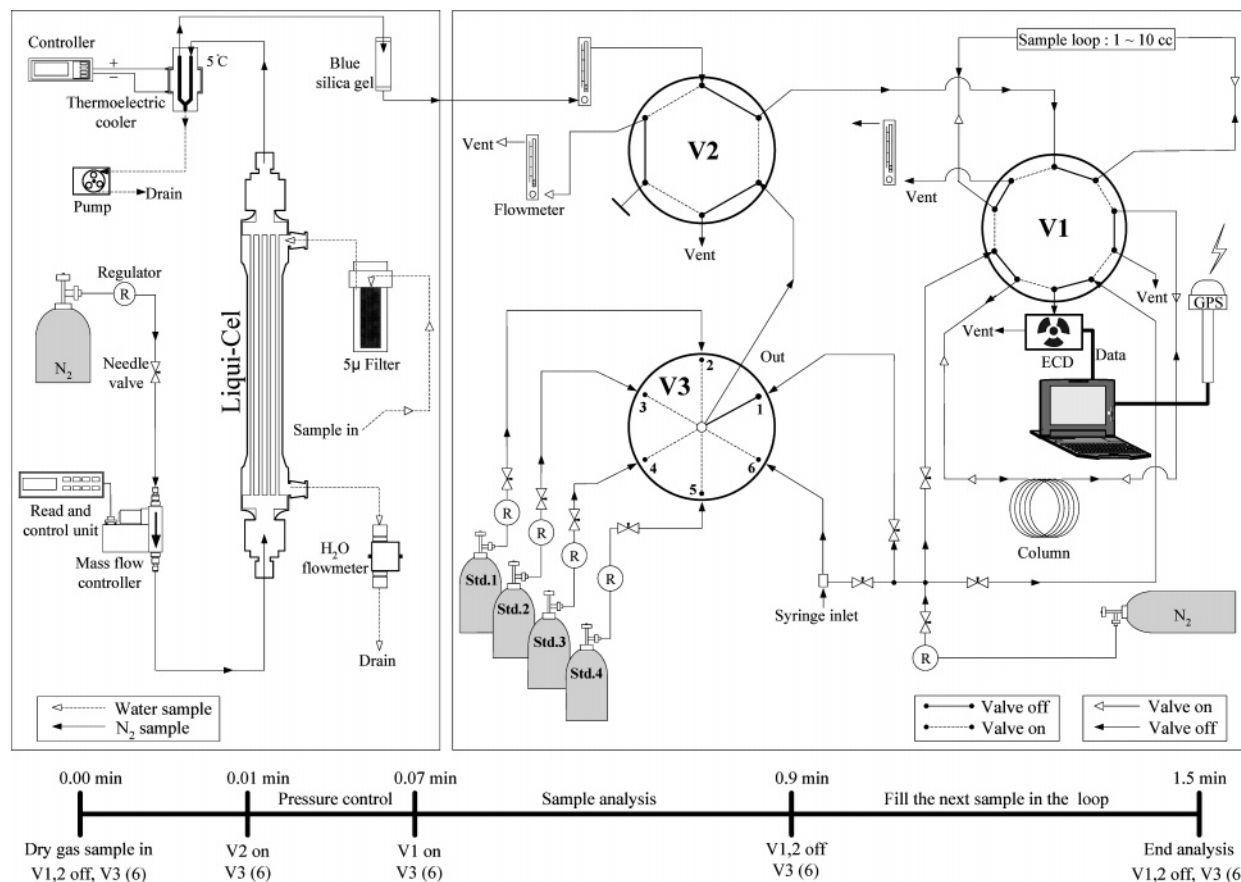


**FIGURE 1.** Schematic representation of the fully automated analytical system for  $\text{SF}_6$ . The  $\text{N}_2$  sweep gas and seawater flows are depicted in the left panel with solid and dotted arrow lines, respectively. In the right panel, valves are shown by letters, and two flow arrows are used to indicate gas lines in which the flow is reversed by valve switching. A time line showing the sequence of measurement events is given at the bottom.

program, a six-port Valco valve (V2 in Figure 1) samples standards and  $\text{SF}_6$  derived from the seawater stream at 1.5-min intervals. The rapid and accurate analysis of  $\text{SF}_6$  is facilitated by the use of a highly efficient gas-stripping device and, to a less extent, by the low solubility of  $\text{SF}_6$  in seawater. A detailed description of the components is given below.

**Rapid and Efficient Extraction System for  $\text{SF}_6$ .** The Liqui-Cel membrane contactor (Celgard) is designed to transfer  $\text{SF}_6$  from the liquid to the gas phase without dispersion. This device is an assemblage of parallel microporous hollow polypropylene fibers bound into an array set around a distribution tube. The minute hollow fibers (i.d. = 220  $\mu\text{m}$ ) are hydrophobic, allowing gases only to pass through the wall pores of the fibers. Within the Liqui-Cel, ultrapure  $\text{N}_2$  extracts  $\text{SF}_6$  and other dissolved gases from the seawater stream until the partial pressure of  $\text{SF}_6$  in the carrier gas is equal to that in the seawater stream. This equilibration system has ancillary components, including a custom-made thermoelectric cooler (24 V and 3 A) and a drying tube for the desiccation of the sampled gas (see Figure 1). The cold trap system includes a thermoelectric module (Acetec), a finned heat exchanger, a cold block, and insulation material. The thermoelectric module consists of an array of semiconductor couples connected electrically in series and thermally in parallel. With a dc potential applied, heat is absorbed at one side of the module, thus cooling it, while heat is rejected at the other side, where the temperature rises. This thermoelectric cooler maintains a cold-side temperature of  $\sim 5^\circ\text{C}$ .

Seawater is continuously pumped from the ship's seawater intake to the outside surface of the aggregated hollow fibers, while ultrapure  $\text{N}_2$  gas simultaneously flows in the opposite direction to the seawater stream, through the inside of the

**TABLE 1.** Optimal  $\text{SF}_6$  Concentration Ranges versus Various Sizes of Sample Loops

sample loop size (mL)	conc'n range (fM)
1.5	21–10000
3.0	10–5000
5.5	5–2700
10.5	3–1500

fibers. A mass flow controller (BrounKhorst) directs a constant flow of  $\text{N}_2$ . The simultaneous but opposite flows of seawater and the carrier  $\text{N}_2$  gas cause, in their enforced proximity, a change in the partial pressure equilibrium between the liquid and gas phase, creating a driving force to transfer the  $\text{SF}_6$  and other gases from solution in seawater into the gas phase.

To avoid water vapor condensation within the gas sample loop and connecting tubes, the extracted gases, including  $\text{SF}_6$ , pass through a thermoelectric cooler. Condensed water is then slowly drained by a pump. The gases are subsequently admitted through a desiccant tube containing 1-mm-sized silica gel.

**Detection System for Equilibrated  $\text{SF}_6$ .** The dried gas sample containing  $\text{SF}_6$  flushes the sample loop, which is installed in valve 1 (V1 in Figure 1), at a rate of 100  $\text{mL min}^{-1}$  for 36 s. The appropriate loop size varies according to the concentration of sampled  $\text{SF}_6$ : the higher the concentration, the smaller the required sample loop (Table 1). A mass flow controller is used to precisely control the flow rate of the dried gas sample containing  $\text{SF}_6$ . Switching V1 from "off" to "on" allows the oxygen-free  $\text{N}_2$  to transfer the gas content in the sample loop to the stainless steel GC column packed

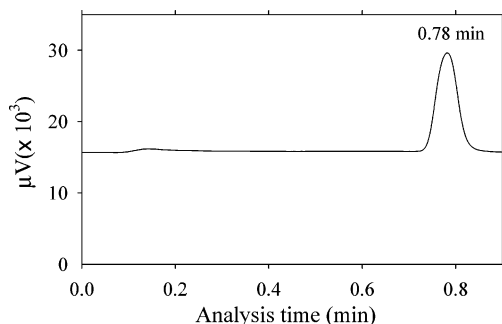


**FIGURE 2.** Chromatogram of 1.5 mL of equilibrated gas after seawater containing 3700 fM of SF<sub>6</sub> is passed through the membrane contactor. The number above the peak is the elution time. The SF<sub>6</sub> elutes at about 0.78 min after sample gas injection into the column.

with a molecular sieve 5A (80/100 mesh, Alltech), in which SF<sub>6</sub> is separated from oxygen and other gases. The ECD is operated at about 300 °C in constant-current mode. Prior to the sample gas injection into the GC, the column is back-flushed with ultrapure N<sub>2</sub> to remove residues from the previous sample, which could otherwise affect the subsequent analysis. Prior to flushing the column, the carrier gas N<sub>2</sub> is passed through molecular sieve and activated charcoal traps to remove any residual oxygen and moisture that might be present. The SF<sub>6</sub> peak appears between 42 and 44 s after sample gas injection into the column (Figure 2). The column is subsequently turned into the backflush mode, and the sample loop is simultaneously placed into the load mode for the next sample by switching V1 from "on" to "off". A complete analytical cycle (see the bottom of Figure 1), from the extraction of SF<sub>6</sub> from the seawater stream to measurement of the SF<sub>6</sub> peak area, takes 1.5 min, which is much faster than in previously documented sparge-trap-based analytical setups (13, 14).

**Calculation.** A fixed volume of ultrapure N<sub>2</sub> rapidly reaches equal partial pressure with the gases dissolved in a stream of seawater flowing through a Liqui-Cel. During the process of partial pressure equilibration, most of the SF<sub>6</sub> dissolved in the seawater is transferred to the gaseous phase. The concentration of SF<sub>6</sub> ([SF<sub>6</sub>]<sub>SW</sub>, mol of SF<sub>6</sub> L<sup>-1</sup>) in seawater prior to equilibration is therefore the sum of the amount of SF<sub>6</sub> present in the gas stream (SF<sub>6</sub>-EXTRT, mol of SF<sub>6</sub>) and that which remained in the seawater stream (SF<sub>6</sub>-RMN, mol of SF<sub>6</sub>):

$$[SF_6]_{SW} = (SF_6\text{-EXTRT} + SF_6\text{-RMN}) / V_{SW} \quad (1)$$

The SF<sub>6</sub>-RMN remaining in the seawater can be obtained if the extraction efficiency of SF<sub>6</sub> (ε) from the seawater sample to the gaseous phase is known. Therefore, the concentration of SF<sub>6</sub> dissolved in the seawater sample prior to equilibration can be determined from the following equation:

$$[SF_6]_{SW} = X_{SF_6} [(P_T - P_{H_2O}) / RT] (V_{N_2} / V_{SW}) (100 / \epsilon) \quad (2)$$

Here  $X_{SF_6}$  is measured SF<sub>6</sub> mole fraction of the dried gas sample,  $P_T$  is the atmospheric pressure in atm,  $P_{H_2O}$  is the vapor pressure of water in atm at the sea surface temperature and salinity,  $V_{N_2}$  is the flow rate of the stripping gas (L min<sup>-1</sup>), and  $V_{SW}$  is the flow rate of seawater (L min<sup>-1</sup>). The extraction efficiency of the membrane contactor was determined by comparing the amount of SF<sub>6</sub> extracted from the first extraction of a sample with the total SF<sub>6</sub> extracted from multiple extractions of the same sample until no SF<sub>6</sub> was extracted. A more detailed description of the procedure used to obtain the extraction efficiency is given in the later section.

**Data Acquisition and Display System.** The data acquisition and display system consists of a valve control module including a GPS and a Visual Basic 6.0/Visual C 6.0-based

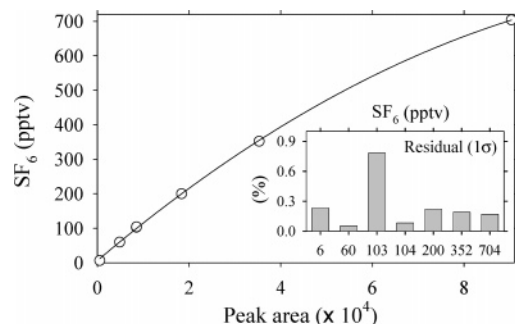


**FIGURE 3.** Calibration curve for the gas chromatograph/electron capture detector (GC-ECD) obtained using a set of SF<sub>6</sub> standards with nominal mixing ratios with N<sub>2</sub> of 6, 60, 103, 104, 200, 352, and 704 pptv. Inset bars represent the standard deviations for four measurements on each standard gas.

program, which directs all analytical sequences, including data acquisition, peak area integration, and data display. This custom-made software provides a virtual interface, comprised of electronic buttons, switches, and a data display for manipulating the instrumentation that drives the automated SF<sub>6</sub> determination system. The graphic display gives a color-coded SF<sub>6</sub> concentration-location (latitude and longitude) plot, which provides the operator with real-time feedback on the distribution and concentration of SF<sub>6</sub> within a patch of water.

## Results and Discussion

**Calibration of the GC-ECD.** The response of the GC-ECD detector is calibrated to gas standards with accurately known mole fractions of SF<sub>6</sub>. Scott Specialty Gases prepared a set of high-pressure SF<sub>6</sub> standards using N<sub>2</sub> as the balance gas with mixing ratios of 6.2, 59.7, 103, 104, 200, 352, and 704 pptv. The standards were prepared in 42-L aluminum cylinders. This range of standards, when used in conjunction with appropriately sized sample loops, encompasses the range of SF<sub>6</sub> concentrations encountered in experimentally injected patches of SF<sub>6</sub> (Table 1). The complete set of standards was analyzed four times within a 2-day period to evaluate the detector response. The detector response increased approximately linearly with increasing SF<sub>6</sub> concentrations for concentrations up to 300 pptv, as observed previously by other investigators (13, 14). For concentrations higher than this range, the response increased nonlinearly with the amount of SF<sub>6</sub> injected (Figure 3). For all the gas standards, the precision was better than 0.2% over a 2-day period, with no visible drift in the detector response over that time. To evaluate the detector response during the field operations, a four-point calibration curve fitted to a second-order polynomial function was used. Usually, a new calibration curve was obtained at the beginning of each hourly cycle of analysis.

**Optimizing the Extraction Efficiency of the Membrane Contactor.** Two important properties of a membrane contactor that should be characterized before use are the optimal extraction efficiency and the equilibration time, the time required to reach the optimal extraction efficiency. The efficiency of SF<sub>6</sub> extraction from a seawater stream largely depends on the ratio of its flow to that of the N<sub>2</sub> sweep gas. Over a wide range of flow rates of the seawater sample and the N<sub>2</sub> sweeping gas, we tested two types of membrane contactor, one with a nominal water volume of 20 mL and another with a nominal volume of 400 mL. To determine the SF<sub>6</sub> extraction efficiency of the small membrane contactor, a 20-L collapsible container was filled with seawater containing spiked SF<sub>6</sub>. This SF<sub>6</sub>-spiked seawater was then pumped through a membrane contactor and subsequently transferred into another collapsible container. The SF<sub>6</sub>



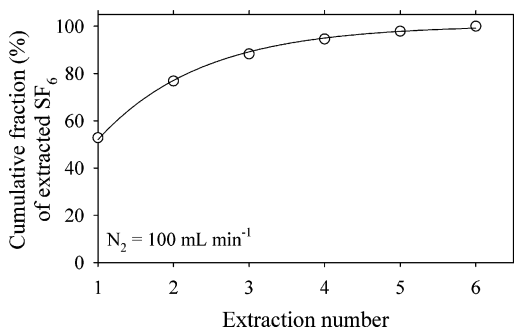


**FIGURE 4.** Cumulative amount ( $\sum_{n=1}^{10} [\text{SF}_6\text{-EXTRT}]_n / [\text{SF}_6\text{-TOTAL}]$ ) of extracted SF<sub>6</sub> (SF<sub>6</sub>-EXTRT) relative to the original amount (SF<sub>6</sub>-TOTAL) as a function of number of extractions ( $n$ ). In this experiment, the sample flow rate of  $\sim 500 \text{ mL min}^{-1}$  and the N<sub>2</sub> sweep gas flow rate of  $\sim 100 \text{ mL min}^{-1}$  were used.

remaining in the seawater sample was further extracted by transferring the seawater sample back into the original collapsible container through the membrane contactor. This extraction cycle continued via transferring the seawater sample back and forth between the two collapsible containers through the membrane contactor until SF<sub>6</sub> was no longer detected. Finally, the SF<sub>6</sub> extraction efficiency of the membrane contactor was determined by comparing the amount of SF<sub>6</sub> extracted from the first extraction cycle of the sample with the total SF<sub>6</sub> extracted from multiple extractions of the same sample. Approximately 7–10 extraction cycles were needed to extract more than 99% of the total amount of SF<sub>6</sub> dissolved in a seawater sample (Figure 4). The extraction efficiency of the large membrane contactor was tested using an identical experimental protocol, except that 500-L rather than 20-L plastic containers were used.

A series of laboratory tests using the small membrane contactor were conducted to determine the optimal combination of flow rates of the N<sub>2</sub> sweep gas and seawater sample. Sweep gas flow rates lower than  $50 \text{ mL min}^{-1}$  were not sufficiently powerful to maintain a constant flow rate sweeping through the Liqui-Cel, largely due to resistance caused by the seawater streamflowing against the sweep gas flow. By contrast, N<sub>2</sub> flow rates greater than  $100 \text{ mL min}^{-1}$  were sufficiently strong to maintain constant flow, but the extracted SF<sub>6</sub> concentration was diluted, resulting in a decrease in the detection ability of the GC-ECD. Consequently, sweep gas flow rates higher than  $100 \text{ mL min}^{-1}$  did not significantly improve the extraction efficiency (Figure 5a). Our laboratory experiments showed that the optimal combination was a seawater flow rate of  $500 \text{ mL min}^{-1}$  and a sweep gas flow rate of  $100 \text{ mL min}^{-1}$ ; this combination yielded a stripping efficiency of approximately 55%; that is, on average 55% of the total SF<sub>6</sub> dissolved in the seawater sample was extracted during the first extraction cycle (Figure 5a). For a given N<sub>2</sub> flow rate, water flow rates lower than  $500 \text{ mL min}^{-1}$  yielded higher SF<sub>6</sub> extraction efficiency than did the water flow rate of  $500 \text{ mL min}^{-1}$  (Figure 5b). However, the water flow rate of  $500 \text{ mL min}^{-1}$  was chosen as the optimal flow rate because water flow rates higher than  $400 \text{ mL min}^{-1}$  yielded a minimal carry-over effect (see Figure 7). The carry-over effect should also be considered in determining the optimal sweep gas flow rate and is discussed in the subsequent section.

The large membrane contactor was set with a seawater flow rate of  $4 \text{ L min}^{-1}$ ; hence, the optimal flow rate ratio was determined by optimizing the flow rate of N<sub>2</sub>. A series of laboratory tests showed  $100 \text{ mL min}^{-1}$  to be the optimal flow rate of the N<sub>2</sub> sweep gas (Figure 5a). This flow rate ratio yielded a stripping efficiency of  $\sim 55\%$ . N<sub>2</sub> sweep gas flow rates lower or greater than  $100 \text{ mL min}^{-1}$  resulted in problems

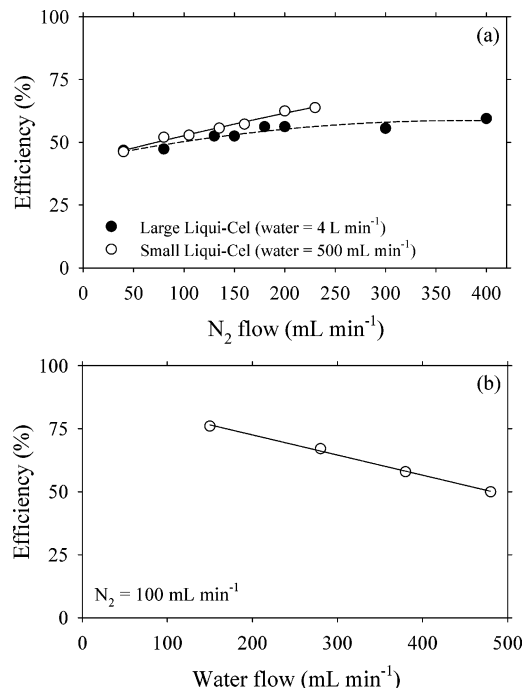


**FIGURE 5.** Extraction efficiency of a small membrane contactor (open circles) with a nominal volume of 20 mL as a function of (a) N<sub>2</sub> flow rate and of (b) water sample flow rate. The water sample flow rate used in (a) was  $\sim 500 \text{ mL min}^{-1}$ , and the N<sub>2</sub> flow rate used in (b) was  $\sim 100 \text{ mL min}^{-1}$ . Shown in (a) is also extraction efficiency of a large membrane contactor (filled circles) with a nominal volume of 400 mL as a function of N<sub>2</sub> flow rate. The large membrane contactor was set with a seawater flow rate of 4–5 L min<sup>-1</sup>.

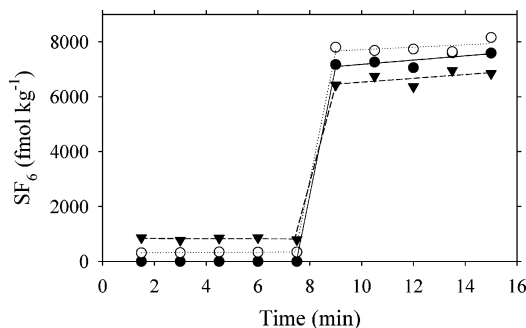


**FIGURE 6.** Analysis of seawater samples containing background or low (350 and 850 fM) SF<sub>6</sub> concentrations followed by SF<sub>6</sub>-spiked (6500–7800 fM) samples. Each symbol represents a set of low (or background) and SF<sub>6</sub>-spiked samples. Filled and open circles and reverse triangles represent a set of background–7300, 300–7800, and 850–6500 fM, respectively.

similar to those encountered when the smaller extraction unit is used. Experiments using the large membrane contactor adopted the same SF<sub>6</sub> extraction method that was used in the small membrane contactor-based experiments, as described in the preceding paragraph.

For the small membrane contactor, the equilibration time was determined by analyzing samples containing low SF<sub>6</sub> concentrations followed by samples containing SF<sub>6</sub> concentrations that are 2–5 orders of magnitude higher than those of the preceding samples. For all three cases, less than 1.5 min was taken to reach the optimal extraction efficiency ( $\sim 55\%$ ) of the membrane contactor after switching from a sample containing a background or low SF<sub>6</sub> concentration to a high SF<sub>6</sub> concentration sample (Figure 6). These results suggest that the complete equilibration between the SF<sub>6</sub>-free carrier N<sub>2</sub> and the SF<sub>6</sub>-spiked seawater stream can be achieved using the membrane contactor within 1.5 min.

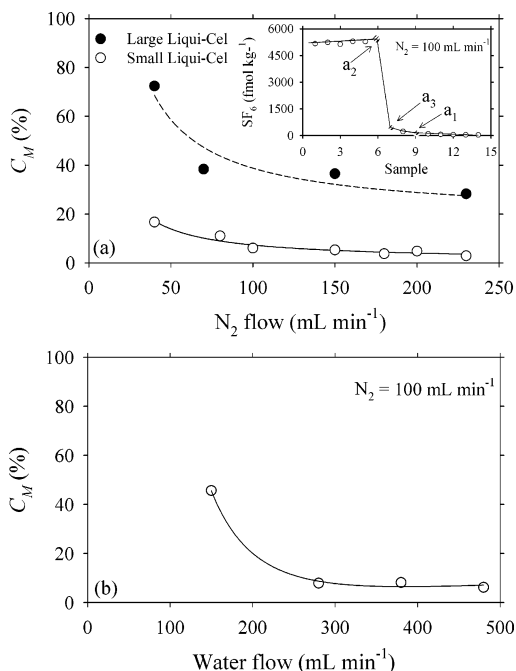


**FIGURE 7. (a) Memory effect coefficients ( $C_M$ , %) of the small (open circles) and large (filled circles) membrane contactors as a function of the flow rate of  $N_2$  gas. In the inset,  $a_1$  is the  $\text{SF}_6$  concentration of the freshwater sample (near background concentration),  $a_2$  is the  $\text{SF}_6$  concentration of the  $\text{SF}_6$  spiked water sample, and  $a_3$  is the  $\text{SF}_6$  concentration of the freshwater sample analyzed immediately following the spiked sample. (b) For a fixed  $N_2$  flow rate ( $\sim 100 \text{ mL min}^{-1}$ ), the memory effect of the small membrane contactor as a function of water sample flow rate ( $\text{mL min}^{-1}$ ).**

**Effect of Carry-Over.** The “memory effect”, whereby contamination from a preceding sample affects the analysis of a subsequent sample, is evident either when high  $\text{SF}_6$  concentrations are followed by lower concentrations or by background concentrations. Thus, during the continuous mode of  $\text{SF}_6$  analysis, the memory effect should be kept to a minimum. In this work, the magnitude of this carry-over effect was evaluated by analyzing  $\text{SF}_6$ -spiked samples followed by freshwater samples containing the background  $\text{SF}_6$  concentration. The  $\text{SF}_6$  concentrations of the  $\text{SF}_6$ -spiked seawater samples were 3–5 orders of magnitude higher than the background  $\text{SF}_6$  concentration. A memory effect coefficient ( $C_M$ ), the fraction of  $\text{SF}_6$  transferred from a preceding high concentration sample, was calculated by using the following equation (15):

$$C_M = [(a_3 - a_1)/(a_2 - a_1)] \times 100 \quad (3)$$

Here  $a_1$  is the  $\text{SF}_6$  concentration of the freshwater sample (near background concentration),  $a_2$  is the  $\text{SF}_6$  concentration of the  $\text{SF}_6$ -spiked water sample, and  $a_3$  is the  $\text{SF}_6$  concentration of the freshwater sample analyzed immediately after the spiked sample. Experiments using the small membrane contactor yielded a memory effect coefficient of 5–10% when  $N_2$  flow rates higher than  $80 \text{ mL min}^{-1}$  and a water flow rate of  $500 \text{ mL min}^{-1}$  were used (Figure 7a,b). By contrast, the large membrane contactor exhibited a memory coefficient of  $\sim 40\%$  or greater for sweep gas flow rates ranging from 40 to  $230 \text{ mL min}^{-1}$  and a water flow rate of  $4 \text{ L min}^{-1}$ . Thus, the memory effect is stronger for the large membrane contactor than for the small one. After the switch from a high  $\text{SF}_6$  concentration to a background level, the contamination from the high  $\text{SF}_6$  concentration of the preceding sample persisted for a few samples (Figure 7a).

The memory effect is of particular concern at the boundary between the  $\text{SF}_6$  patch and the  $\text{SF}_6$ -free surrounding water.

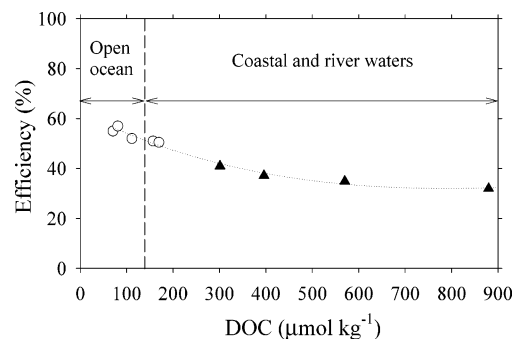


**FIGURE 8.  $\text{SF}_6$  extraction efficiency of the small membrane contactor as a function of dissolved organic carbon concentration (DOC) ( $\mu\text{mol kg}^{-1}$ ).**

When samples at such boundaries are analyzed, high  $\text{SF}_6$  concentrations may be followed by background concentrations and, as a consequence, the memory effect may extend the tail of the tracer distribution to longer than its actual length, resulting in an overestimation of the patch size. The e-folding time for the memory effect was estimated to be 3–4 min, indicating that the length of the patch can be overestimated by  $\sim 0.5 \text{ km}$  at the average boat speed of  $10 \text{ km h}^{-1}$ . However, the memory effect produced by the small membrane contactor does not greatly detract from the accurate definition of the temporal or spatial change in an enhanced patch of  $\text{SF}_6$ .

**Effect of Surfactant on the Extraction Efficiency of the Membrane Contactor.** The extraction efficiency of the membrane contactor generally deteriorates with time as particles and surfactants are progressively deposited on the surface of the membrane contactor. This effect is reduced by installing a  $5 \mu\text{m}$  pore-sized filtration device upstream of the membrane contactor to remove organic and inorganic particles; however, this does not remove surfactants. In this study, dissolved organic carbon (DOC) was used as a proxy for surfactants in seawater because surfactant concentrations are strongly correlated with DOC concentrations (16). Therefore, the effect of surfactants on  $\text{SF}_6$  extraction efficiency was evaluated by measuring the  $\text{SF}_6$  extraction efficiency of the membrane contactor as a function of DOC concentration. The soluble surfactant Triton X-100 was used in this experiment due to its similarity to natural surfactants found in the marine environment (17). A series of experiments were conducted at DOC concentrations ranging from 50 to  $880 \mu\text{M}$ , which encompasses the range encountered in marine environment. In these laboratory tests, natural seawater samples were used for DOC concentrations lower than  $150 \mu\text{M}$  whereas samples with DOC concentrations higher than  $150 \mu\text{M}$  were prepared by adding Triton X-100 to natural seawaters. The results showed that DOC concentrations of 50– $120 \mu\text{M}$  caused only a slight decrease in  $\text{SF}_6$  extraction efficiency but that further increase of the DOC concentration led to a significant deterioration in extraction efficiency (Figure 8).

To minimize the effect of DOC on  $\text{SF}_6$  extraction efficiency, the membrane contactor is cleaned by circulating a 2 wt % KOH solution through the device for 20 min followed by flushing with a 2 wt % phosphoric acid solution for the same time. The membrane contactor is then thoroughly rinsed with ambient distilled water for 20 min until a neutral pH is achieved. This cleaning protocol was followed once during the 4-day field experiment carried out in biologically prolific coastal waters, as described in the subsequent section. Weekly cleaning was sufficient to maintain the extraction efficiency.

**Tracing a Patch of Harmful Algal Bloom (HAB) Infected Water.** The  $\text{SF}_6$  underway system described in this article can trace the  $\text{SF}_6$  patch until the mixed layer  $\text{SF}_6$  concentra-

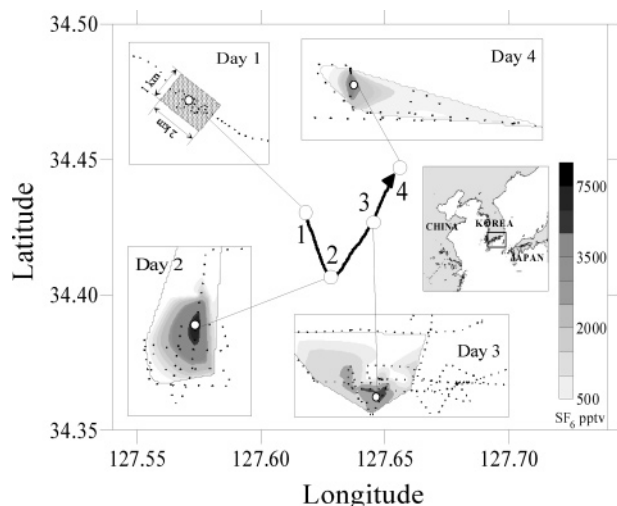


**FIGURE 9. Temporal evolution of SF<sub>6</sub> concentration over the 4-day period of the Lagrangian experiment that was carried out in the southern coastal waters of Korea (34.42° N and 127.63° W) in August 2003.**

tions decrease to the detection limit of <5 fM. The temporal evolution of SF<sub>6</sub> concentrations in the surface mixed layer is largely governed by air–sea gas exchange, horizontal diffusion, and deepening of the mixed layer (6, 18). Therefore, the intensities of these processes determine the length of survey time. In the surface marine environments, the SF<sub>6</sub> injection into the mixed layer allows one to trace the SF<sub>6</sub>-labeled patch of water usually longer than 3 weeks (9–12).

The automated SF<sub>6</sub> detection system described above was used to trace a patch of seawater containing *Cochlodinium polykrikoides*, which regularly causes harmful algal blooms in the coastal waters of southern Korea (Figure 9). A total of 2.74 mol of SF<sub>6</sub> was released at a depth of 5 m by bubbling the gas into the water column through a 0.5 mm porous tube, over an area of 2 km by 1 km width. A GPS buoy was simultaneously deployed to follow the movement of the SF<sub>6</sub> patch. Each daily survey started with the locating of the GPS buoy, which was usually found near the SF<sub>6</sub> patch. Once the patch was located, the data acquisition/display system continuously recorded the peak area of each SF<sub>6</sub> measurement and the corresponding sampling location given by the GPS. The results were plotted on the screen in near-real time, and a map of the tracer patch was developed; this map was used to direct the ship's course during sampling.

Daily mapping of the spatial extent of the SF<sub>6</sub>-labeled water mass indicated that the patch was coherent over a 4-day period and moved less than 8 km from the injection point. During the 4-day tracer experiment, a suite of hydrographic, chemical, and biological measurements (temperature, salinity, nutrients, and algal abundance) were taken each day at vertical profile stations inside the patch, to monitor changes in physical environment and the algal population. The resulting data suggest that in situ growth of *C. polykrikoides* within the SF<sub>6</sub>-labeled water accounts for only a fraction of the total cell increase. Results obtained from this SF<sub>6</sub> Lagrangian experiment are discussed in detail elsewhere (18), and possible mechanisms for bloom initiation and accumulation at the study site are also presented (18).

In summary, the underway SF<sub>6</sub> detection system fitted with a Liqui-Cel membrane contactor extraction device described in this paper has proved to be an efficient and rapid method for extracting and quantifying SF<sub>6</sub> in a seawater stream and enables near real-time monitoring of the location-SF<sub>6</sub> concentration plot on-screen. The advantages of the automated system include the ability to rapidly and accurately analyze multiple samples (1.5 min/sample), a low detection

limit (<5 fM), and automated collection and display of data. The analysis system requires minimal daily maintenance and can provide reliable data on the concentration of SF<sub>6</sub> injected into a marine surface mixed layer. The SF<sub>6</sub> detection method described here will find increasing use in the study of biogeochemical processes in the marine environment.

## Acknowledgments

The success of this field experiment conducted in the coastal waters of the southern Korea in August 2003 can be attributed to the hard work of the participants and the crew of National Fisheries and Development Institute R/V TAMGU-7. K.L.'s interactions with Dr. R. Wanninkhof and C. Neill during his tenure in Dr. R. Wanninkhof's laboratory of the Atlantic Oceanographic and Meteorological Laboratory as a post-doctoral research associate were helpful in the early stage of developing the system. This work was financially supported by the Korea Aerospace Research Institute and the National Research Laboratory (NRL) Program (2005) of the Korea Science and Engineering Foundation. Partial support was also provided by the AEBRC at POSTECH, the Brain Korea 21 Project, and the KOSEF through Grant No. R01-2002-000-00549-0 (2005).

## Literature Cited

- (1) Ho, D. T.; Schlosser, P.; Caplow, T. E. Determination of longitudinal dispersion coefficient and net advection in the tidal Hudson river with a large-scale, high-resolution SF<sub>6</sub> tracer release experiment. *Environ. Sci. Technol.* **2002**, *36*, 3234.
- (2) Wanninkhof, R.; Sullivan, K. F.; Top, Z. Air-sea gas transfer in the Southern Ocean. *J. Geophys. Res.* **2004**, *109*, doi: 10.1029/2003JC001767.
- (3) Ravishankara, A. R.; Solomon, S.; Turnispeed, A. A.; Warren, R. F. Atmospheric lifetimes of long-lived halogenated species. *Science* **1993**, *259*, 194.
- (4) Maiss, M.; Brenninkmeijer, C. A. M. Atmospheric SF<sub>6</sub>: trends, sources, and prospects. *Environ. Sci. Technol.* **1998**, *32*, 3077.
- (5) Bullister, J. L.; Wisegarver, D. P.; Menzia, F. A. The solubility of sulfur hexafluoride in water and seawater. *Deep-Sea Res., Part 1* **2002**, *49*, 175.
- (6) Stanton, T.; Law, C. S.; Watson, A. J. Physical evolution of the IRONEX-1 open ocean tracer patch. *Deep-Sea Res., Part 2* **1998**, *45*, 947.
- (7) Wanninkhof, R.; Ledwell, J. L.; Broecker, W. S. Gas Exchange-wind speed relationship measured with sulfur hexafluoride on a lake. *Science* **1985**, *227*, 1224.
- (8) Ledwell, J. R.; Watson, A. J.; Law, C. S. Mixing of a tracer in the pycnocline. *J. Geophys. Res.* **1998**, *103*, 21499.
- (9) Martin, J. H.; Coale, K. H.; Johnson, K. S.; Fitzwater, S. E.; Gordon, R. M.; Tanner, S. J.; Hunter, C. N.; Elrod, V. A.; Nowicki, J. L.; Coley, T. L.; Barber, R. T.; Lindley, S.; Watson, A. J.; Scoy, K. Van; Law, C. S.; Liddicoat, M. I.; Ling, R.; Stanton, T.; Stockel, J.; Collins, C.; Anderson, A.; Bidigare, R.; Ondrusek, M.; Latasa, M.; Millero, F. J.; Lee, K.; Yao, W.; Zhang, J. Z.; Friederich, G.; Sakamoto, C.; Chavez, F.; Buck, K.; Kolber, Z.; Greene, R.; Falkowski, P.; Chisholm, S. W.; Hoge, F.; Swift, R.; Yungel, J.; Turner, S.; Nightingale, P.; Hatton, A.; Liss, P.; Tindale, N. W. Testing the iron hypothesis in ecosystems of the equatorial Pacific Ocean. *Nature* **1994**, *371*, 123.
- (10) Coale, K. H.; Johnson, K. S.; Fitzwater, S. E.; Gordon, R. M.; Tanner, S.; Chavez, F. P.; Ferioli, L.; Sakamoto, C.; Rogers, P.; Millero, F.; Steinberg, P.; Nightingale, P.; Cooper, D.; Cochlan, W. P.; Landry, M. R.; Constantinou, J.; Rollwagen, G.; Travnica, A.; Kudela, R. A massive phytoplankton bloom induced by an ecosystem-scale iron fertilization experiment in the equatorial Pacific Ocean. *Nature* **1996**, *383*, 495.
- (11) Boyd, P. W.; Watson, A. J.; Law, C. S.; Abraham, E. R.; Trull, T.; Murdoch, C. E.; Bakker, D. C. E.; Bowie, A. R.; Busseler, K. O.; Chang, H.; Charette, M.; Croot, P.; Dowling, K.; Frew, R.; Gall, M.; Hadfield, M.; Hall, J.; Harvey, M.; Jameson, G.; LaRoche, J.; Liddicoat, M.; Ling, R.; Maldonado, M. T.; McKacy, R. M.; Nodder, S.; Pickmer, S.; Pridmore, R.; Rintoul, S.; Safi, K.; Sutton, P.; Sterzerpek, R.; Tenneberger, K.; Turner, S.; Waite, A.; Zeldis, J. A mesoscale phytoplankton bloom in the polar Southern Ocean stimulated by iron fertilization. *Nature* **2000**, *407*, 695.

- (12) Boyd, P. W.; Law, C. S.; Wong, C. S.; Nojiri, Y.; Tsuda, A.; Levasseur, M.; Takeda, S.; Rividin, R.; Harrision, P. J.; Strzepoek, R.; Gower, J.; Mvkay, R. M.; Abaraham, E.; Arychuk, M.; Barwell-Clarke, J.; Crawford, W.; Crawford, D.; Hale, M.; Harada, K.; Johson, K.; Kiyosawa, H.; Kudo, I.; Marchetti, A.; Miller, W.; Needoba, J.; Nishioka, J.; Ogawa, H.; Page, J.; Robert, M.; Satio, H.; Sastri, A.; Sherry, N.; Soutar, T.; Sutherland, N.; Taira, Y.; Whitney, F.; Wong, S. E.; Yoshimura, T. The decline and fate of an iron-induced subarctic phytoplankton bloom. *Nature* **2004**, *428*, 549.
- (13) Upstill-Goddard, R. C.; Watson, A. J.; Wood, J.; Liddicoat, M. I. Sulphur hexafluoride and helium-3 as seawater tracers: deployment techniques and continuous underway analysis for sulphur hexafluoride. *Anal. Chim. Acta* **1991**, *249*, 555.
- (14) Law, C. S.; Watson, A. J.; Liddicoat, M. I. Automated vacuum analysis of sulphur hexafluoride in seawater; derivation of the atmospheric trend 1970–1993 and potential as a transient tracer. *Mar. Chem.* **1994**, *48*, 57.
- (15) Guihua, L.; Wie, B. J. V.; Leatzow, D.; Weyrauch, B.; Tiffany, T. Experimental design modeling of carryover to optimize air-segmented continuous flow analysis. *Mar. Chim. Acta* **2000**, *408*, 21.
- (16) Frew, N. M.; Nelson, R. K.; McGillis, W. R.; Edson, J. B. Spatial variations in surface microlayer surfactants and their role in modulating air-sea exchange. *Geophys. Monogr.* **2002**, *127*, 153.
- (17) Saylor, J. R. The fate of soluble and insoluble surfactant monolayers subjected to drop impacts. *Exp. Fluids* **2003**, *34*, 540.
- (18) Park, G.-H.; Lee, K.; Koo, C.-M.; Lee, H.-W.; Lee, C. K.; Koo, J. S.; Lee, D.; Shin, S.-H.; Kim, H. G.; Park, B. K. A sulfur hexafluoride-based Lagrangian study on initiation and accumulation of the red tide *Cochlodinium* in southern coastal waters of Korea. *Limnol. Oceanogr.* **2005**, *50*, 578.

*Received for review January 24, 2005. Revised manuscript received August 22, 2005. Accepted August 24, 2005.*

ES050149G